5

Nanocomposite materials for 3D printing

Hoon Kim[1, 2], Tanveer Ahmed Khan[2], Kwang-Hyun Ryu[2], In-Sung Sohn[1], Hyun-Joong Kim[2*]

[1]Graphy R&D Center, Graphy Inc., Seoul 08501, Republic of Korea
[2]Lab. Of Adhesion & Bio-Composite, Program in Environmental Materials Science, College of Agriculture & Life Sciences, Seoul National University, Seoul 08826, Republic of Korea

Outline

Introduction

3D printing is an additive manufacturing (AM) technique for fabricating a wide range of structures and complex geometries from 3D model data. The process consists of printing successive layers of materials that are formed on top of each other. The technology was developed by Charles Hull in 1986 using stereolithography (SLA), and subsequently developed to include powder bed fusion, fused deposition modelling (FDM), inkjet printing, and contour crafting (CC). 3D printing, which involves various methods, materials, and equipment, has evolved over the years, and can be used to transform manufacturing and logistics processes. Additive manufacturing is widely applied in different industries, including construction industries, manufacturing of prototypes, and biomechanical industries. [1] As AM technology develops, efforts have been made to apply the technology in several fields, as shown in Figure 5.1.

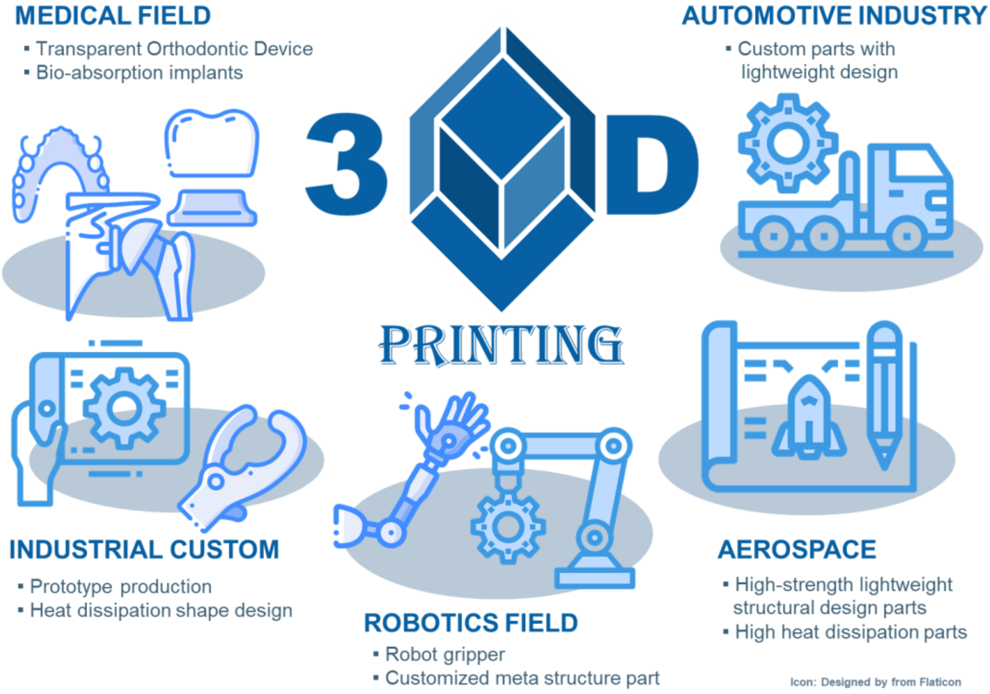

FIGURE 5.1
Application of 3D printing in different industries [2].

New applications for novel materials are emerging, and AM methods are continuously being developed. One of the main drivers for this technology to become more accessible is the expiry of earlier patents, which has given manufacturers the capability to develop new 3D printing devices. Recent developments have reduced the cost of 3D printers, thereby expanding their application in schools, homes, libraries, and laboratories. Initially, 3D printing was extensively used by architects and designers to produce aesthetic and functional prototypes owing to its rapid and cost-effective prototyping capabilities. The use of 3D printing minimises additional expenses incurred during product development. However, in the past few years, 3D printing has been fully utilised in various manufacturing processes, from the production of prototypes to products. Product customisation has been a challenge for manufacturers because of the high cost associated with the production of tailor-made products for end users. In contrast, small quantities of customised products can be 3D printed at relatively low costs using AM. This is specifically useful in the biomedical field, wherein unique patient-customised products are typically required. Customised functional products are gaining attention in the field of 3D printing, as predicted by Wohlers Associates, who envisioned that approximately 50% of 3D printing will involve the manufacturing of commercial products in 2020. [3]

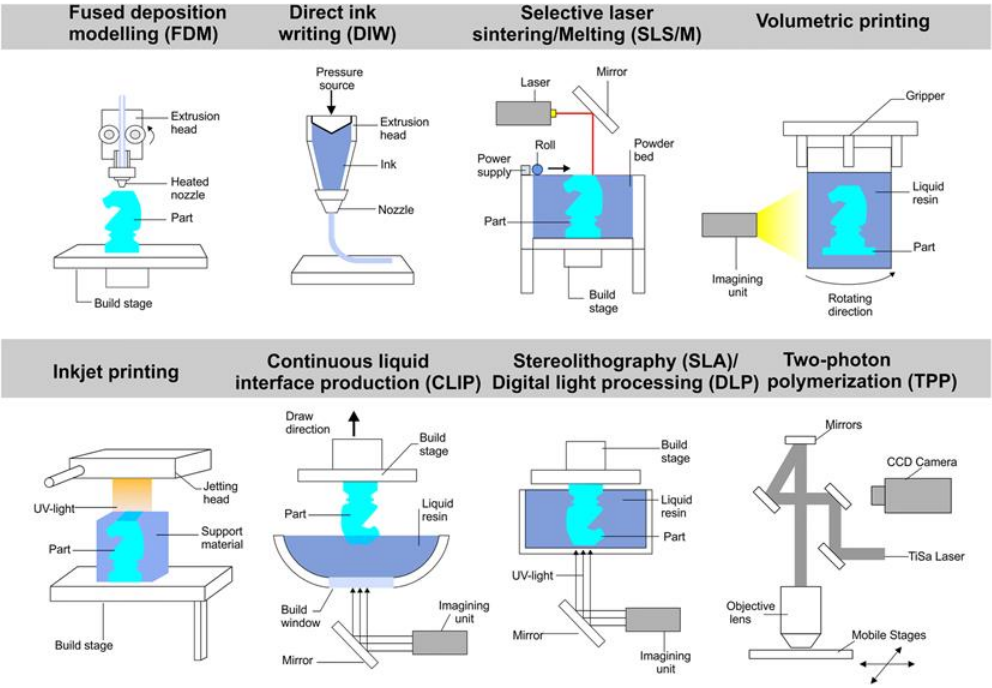

FIGURE 5.2
Schematic summary of the different 3D printing techniques. [4] Reproduced with permission. Copyright 2011, Royal Society of Chemistry.

Mass customisation is an advantage of 3D printing; i.e., each product can be modified according to the user's characteristics while maintaining a low price through mass production. 3D printing has no mould or additional requirements compared to traditional production methods. In addition, as moulds are not required, there is no cost involved in changing the design of the product. Therefore, the advantage of 3D printing is not its lower price with mass production, but its ability to produce various shapes at low prices. However, AM requires further investigation because the high cost and time consumption of the process are not suitable for simple mass production.

A variety of materials, including metals, ceramics, and concrete, can be used in 3D printing. However, this Chapter focuses on the use of polymers in 3D printing.

As shown in Figure 5.2, 3D printing of polymers can be divided into two methods: moulding, in which heat is applied to the polymer, and photocuring, in which a resin with an acrylic functional group is selectively cured by UV irradiation. This Chapter provides details on both methods.

The impact of 3D printing on the 4th industrial revolution and our lives is still unknown. This is because the extent to which the technology can be improved is still unknown. However, various 3D printing methods have already been developed, and further studies are being conducted on a variety of printing methods and their corresponding materials. In the next section, the most representative 3D printing methods will be briefly introduced. 3D printed materials tend to have lower mechanical strength compared to conventional injection-moulded materials. This phenomenon is related to the inevitable structural defects that occur during 3D printing; however, to overcome these limitations, nanocomposite material technology can be applied to 3D printing.

Additive manufacturing (3D printing) has the potential to produce new types of multifunctional nanocomposites. The ability to print complex 3D objects layer by layer provides the opportunity to take advantage of nanomaterial AM to better control material properties at the component level. Functionalisation through the combination of nanomaterials and printing materials can be characterised by increased thermal and electrical conductivity, increased strength, and reduced weight. By applying a new paradigm to nanocomposite functionality, we can discuss the promise of nanomaterial-based AM. [5], [6]

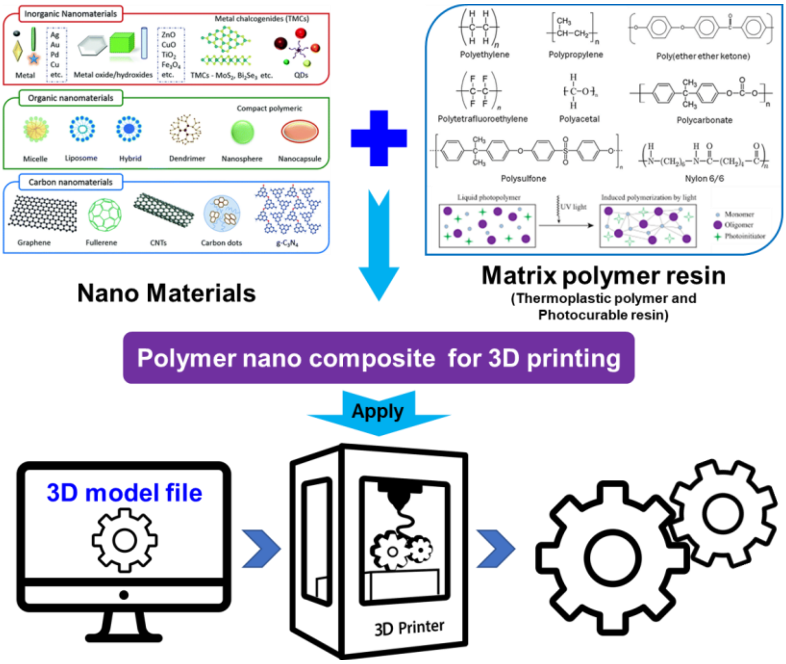

FIGURE 5.3

Conceptual schematic diagram of 3D printing using nanocomposite technology. [7] Reproduced with permission. Copyright 2018, Springer Nature.

Thermal FDM 3D printing

Fused deposition modelling (FDM) is one of the most popular additive manufacturing technologies used in various engineering applications. The FDM process was commercially introduced in the early 1990s by Stratasys Inc., USA. The quality of the FDM processed parts mainly depends on careful selection of the process variables. Thus, identification of FDM process parameters that significantly affect the quality of the FDM processed parts is important. Recently, several methods to improve the mechanical properties and quality of the parts have been investigated using various experimental design techniques and concepts. [8]

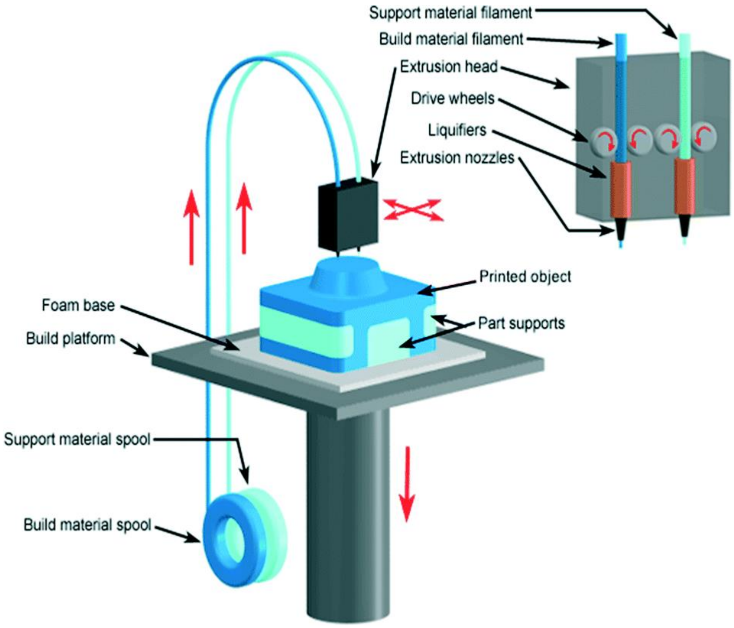

FIGURE 5.4
Schematic diagram of the FDM process. [9] Reproduced with permission. Copyright 2016, Royal Society of Chemistry.

Figure 5.4 shows a schematic diagram of an FDM 3D printer. Essentially, the thermoplastic resin, processed in filament form, is heated near the nozzle, converted into a semi-liquid form, and then extruded. The extruded material is deposited on the printing bed or on a previously printed layer and cooled to convert it from a semi-liquid form to a solid form. Thus, an interface is inevitably created during the printing lamination process. In addition, voids are generated depending on the printing conditions and the interface on which the lamination is formed.

During the lamination process, the interlayer bonding strength of the polymer is affected by a variety of factors, such as the characteristics of the polymer material, output speed, output temperature, bed temperature, chamber temperature, etc. As shown in Figure 5.5, the inter-diffusion and electrical charge of the material also affect the bonding force. [10]

In addition, changes in the states of the polymers lead to material accumulation. Shrunken materials will reduce the completeness and accuracy of the output. However, the main advantage of FDM is its low cost, fast, and facile processing method. The disadvantages of FDM include the weak mechanical properties of the products, low surface resolution, and that a limited number of thermoplastic polymers can be applied because of their low interlayer bond strengths. [11], [12]

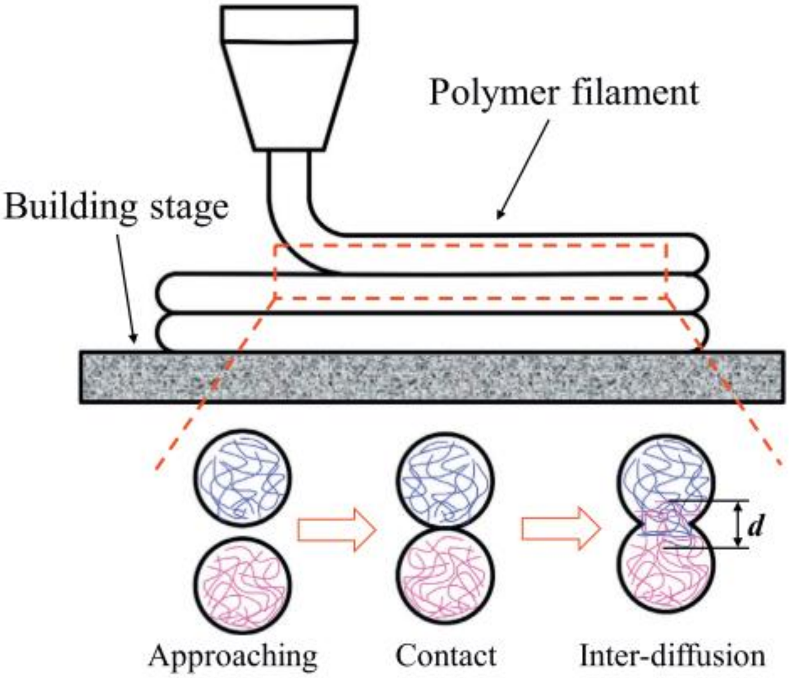

FIGURE 5.5
Inter-molecular diffusion between the polymer fibres during FDM. [11] Reproduced with permission. Copyright 2018, Elsevier Ltd.

UV-assisted 3D printing

Stereolithography (SLA) and digital light projector (DLP) methods

All 3D printing methods that involve radically curing monomers and oligomers containing acrylic functional groups with UV to output a solid state object can be characterized as UV-assisted 3D printing methods. The two most representative types of UV-assisted 3D printing are stereolithography (SLA) and digital light projector (DLP). Different UV irradiation methods, surface irradiation or point irradiation, are used for the two different methods. Furthermore, the printing speed and resolution also depend on the chosen method.

SLA is one of the most accurate AM methods developed and commercialised by 3D Systems in 1986 and has steadily evolved over the past 30 years. [13] Effectively, the DLP method is another type of SLA method. As shown in Figure 5.6, the difference between SLA and DLP is the manner in which the resin layer is cured. In DLP the resin layer is cured all at once by projecting a 2D UV plane pattern, while in SLA the point where the UV laser projects is moved. The DLP method has a faster printing speed than SLA, but a difference in resolution may occur owing to a difference in the light source (laser vs. projection). In DLP-type 3D printers, the high viscosity of the resin used causes poor printing. However, in the dental field, because the size of the material to be printed is small, it is possible to print relatively smoothly, even with high-viscosity resins. As shown in Figure 5.7, in both the DLP and SLA methods the intended product is sliced into a 2D image, and the final output is produced through a layer-by-layer curing process.

In STA, control over the thickness of the cured layer is essential. For a given resin, the cure depth is determined by the energy of the light to which the resin is exposed. This energy can be controlled by adjusting the power of the light source and the scanning speed (for laser systems) or exposure time (for projection systems). The kinetics of the curing reactions are quite complex. Although the different stages of the addition-type polymerisation process (initiation–propagation–termination) can be expressed mathematically, the presence of multifunctional monomers and the transition of the polymerising liquid to a solid complicates its description. [14]

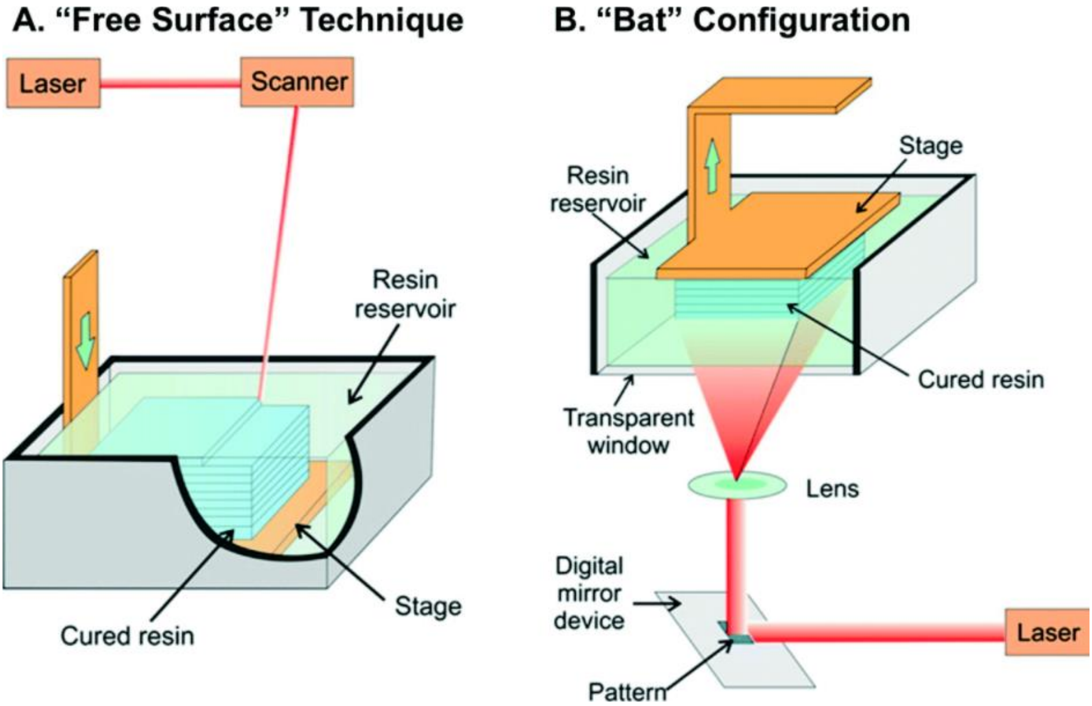

FIGURE 5.6

SL configurations. (A) "free surface" SL technique; (B) "constrained surface" SL technique or the "bat" configuration SL printing. [15] Panels (A) and (B) are reproduced with permission. Copyright 2016, royal society of chemistry.

Xolography

Xolography refers to volumetric 3D materialising technology based on dual-colour photoinitiators. It was first introduced in December 2020 as a dual-colour technique using photoswitchable photoinitiators to induce local polymerisation inside a confined monomer volume upon linear excitation by intersecting light beams of different wavelengths. The concept was demonstrated with a volumetric printer designed to generate 3D objects with complex structural features as well as mechanical and optical functions. Compared to state-of-the-art volumetric printing methods, this techniques has a resolution approximately ten times higher than computed axial lithography without feedback optimisation, and a volume generation rate four to five orders of magnitude higher than that of two-photon photopolymerisation. We expect this technology to transform the rapid volumetric production of objects at the nanoscopic to macroscopic length scales. [16] This new method of bulk 3D printing can produce more precise and complex structures as it does not require the assistive techniques used in existing 3D printing. However, this assumption is only theoretical, as the viscosity of the ink used in the printer must be high for the printed material to stably maintain its structure. In the future, if the printing method is stabilised and suitable printing materials can be secured, it should be a promising technology that can output materials of larger sizes and higher resolutions.

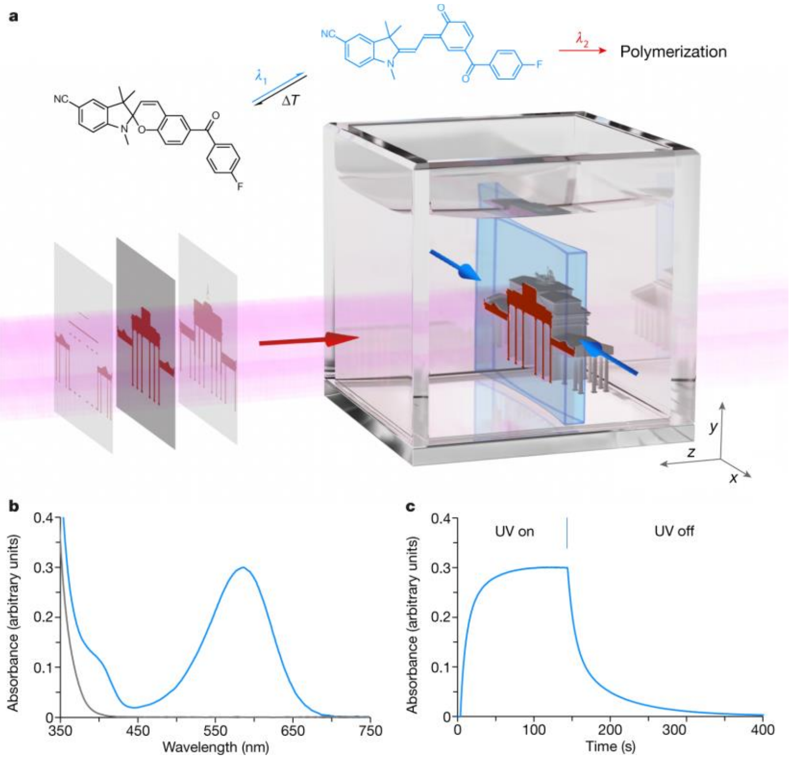

FIGURE 5.8

Overview of xolography-based 3D printing and volumetric digital manufacturing of 3D models. [16] Reproduced with permission. Copyright 2020, Springer Nature.

Thermoplastic biocompatible 3D printing materials

Thermoplastic polymers can be used in FDM and SLA. Materials that can be processed into filaments with uniform diameters, such as polypropylene (PP), acrylonitrile butadiene styrene (ABS), polycarbonate (PC), polyethylene terephthalate (PETG), and polyether ether ketone (PEEK), mostly apply [1], [17–19]. The most recognised biocompatible thermoplastic 3D printing material is poly(lactic acid) (PLA) [20]. It has been attracting more attention than petroleum-derived thermoplastic resins, as it is a sustainable and renewable resource. In addition, because of its biodegradable properties, microplastics are becoming an issue. [21–25] Owing to its biocompatibility and biodegradability, PLA has also commonly been used in biomedical fields. PLA is mechanically strong and hard, however, it is a brittle material with exceptionally low flexibility and impact resistance. Complexation can be used to improve the mechanical properties of the materials and impart functionality. Thus, it is possible to overcome the decrease in mechanical strength of the products caused by defects that occur during the FDM printing process [10], [26], [27]. Based on these properties of PLA, it has been used in the 3D printing of biomaterials as a new tool for the fabrication of scaffolds with well-defined and reproducible architectures. 3D printing technology unlocks the possibility of building custom scaffolds based on patient-specific tissue defects. This technology combines computer design with automatic printing technology. Additionally, temporary custom scaffolds produced by 3D printing provide an excellent in vitro platform for studying the effects of geometry/architecture on cellular responses and computer modelling of scaffold behaviour. In addition, a 3D structure with improved mechanical performance can be obtained. [28] However, to achieve functionality and enhanced mechanical properties, a nanocomposite material must be considered rather than a single material.

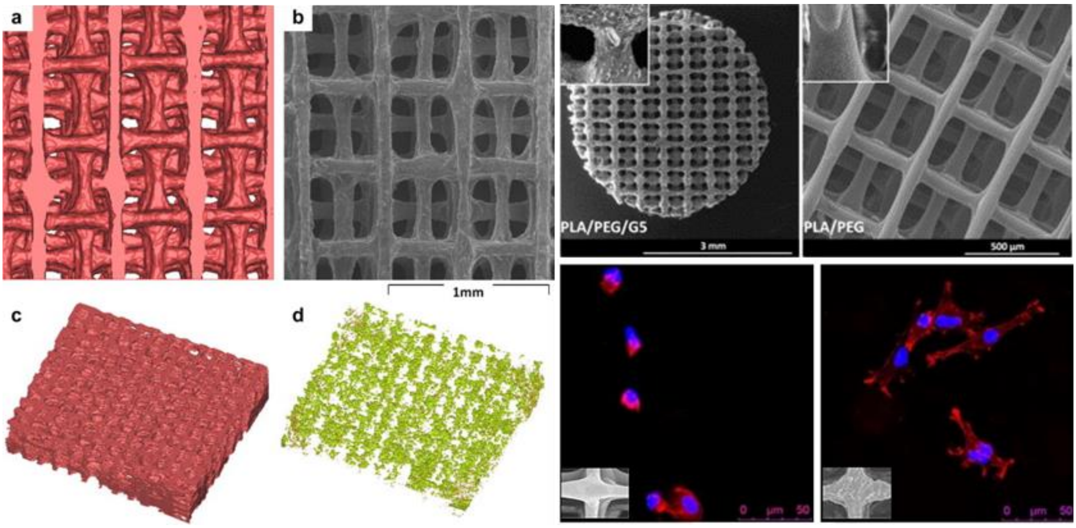

FIGURE 5.9
(a) 3D reconstructed and (b) SEM images of a PLA/PEG/G5 scaffold. 3D reconstructions of an ORTH (c) PLA/PEG/G5 scaffold, and (d) G5 particle distribution within the polymeric matrix. Fluorescence images of attached cells on the PLA/PEG and PLA/PEG/G5 scaffolds are also included. [28] Reproduced with permission. Copyright 2013, Elsevier Ltd.

UV curable 3D printing materials

3D photopolymerisation (also known as photocuring or photo-crosslinking) involves the use of monomers/oligomers in a liquid state that can be cured/photopolymerised upon exposure to a light source of a specific wavelength to produce thermosets. [29] A photoinitiator or photoinitiator system (with relatively high absorption coefficients) is required to convert the photolytic energy into reactive species (radicals or cations), which can drive chain growth via a radical or cationic mechanism. Typically, photoinitiators with high molar extinction coefficients at short wavelengths (mostly UV < 400 nm) are used to initiate the photochemical reactions. [29]

3D photopolymerisation using photocurable resins includes various techniques and mechanisms, as shown in Figure 5.10. However, it mainly involves free radical and cationic reaction mechanisms, and the use of photo-initiators that form radicals on UV light exposure. Resins that require radical initiators for the photoinitiation reaction mainly constitute meth(acrylate) monomers/oligomers, as shown in Figure 5.11. As indicated above, although denoted differently depending on the wavelength of the initial light energy, the radical polymerisation mechanism remains the same. In addition, the 3D printing curing and post-curing conditions should be altered according to the rheological and polymerisation characteristics of the photo-curing resin used. [30]

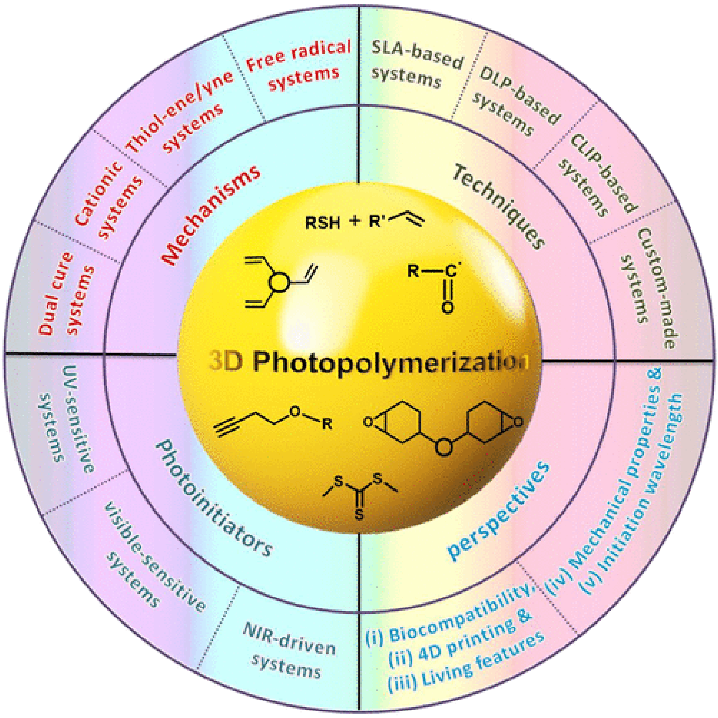

FIGURE 5.10

Schematic diagram of the components and technologies involved in 3D printing photocurable resins. [30] Reproduced with permission. Copyright 2019, American Chemical Society

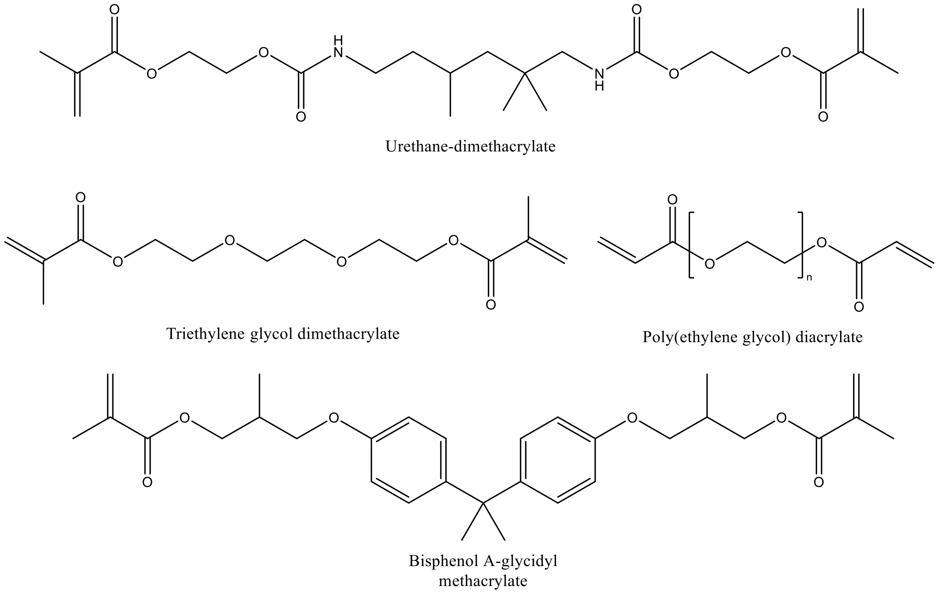

Urethane-dimethacrylate

Triethylene glycol dimethacrylate

Poly(ethylene glycol) diacrylate

Bisphenol A-glycidyl methacrylate

FIGURE 5.11
Examples of meth(acrylate) monomers/oligomers typically used in 3D photopolymerisation. [30]

Nanomaterials for 3D printing

Nanomaterials have attracted attention from academic researchers and industries because they combine the properties of the nanomaterial and the base material matrix. A number of nanomaterials have been used to 3D print polymer nanocomposites. These nanomaterials include graphene, carbon nanotubes (CNTs), carbon nanofibres, nanocellulose, and nanoclays. Carbon is used as a raw material for several commercial products [31–33]; however, nanomaterials, such as graphene and CNTs, are not suited for widespread use, as they are expensive. Nanoclays are more affordable and, therefore, more suitable for industrial applications. [34] Nanomaterials could dramatically improve the properties of materials used in a variety of important industries, such as the medical, automotive, semiconductor, plastics, and chemicals industries. [35] However, several challenges remain for the application of nanocomposites in 3D printing production, including processing, cost, consistency and reliability in volume production, high lead-time, and oxidative and thermal instability of the nanomaterials. New processing techniques with regards to multi-functionality could offer advantages for nanocomposite 3D printing.

Nanoclays are classified according to their elemental composition, electrical charge, and dimensions. They are characterised into several categories depending on their elemental composition, including montmorillonite, smectite, kaolinite, chlorite, and illite. Nanoclays can be divided into cationic and anionic nanoclays. The surface treatment process and surfactant material applied to the nanoclay depend on its electrical charge. Finally, the morphology of the clay can be categorised as nanolayers, nanoparticles, nanotubes, and whiskers. Additionally, clay can be categorised according to their preparation pathway, which includes three types: natural, incidental, and synthetic nanoparticles. [34]

Several types of clay exist, however, clay nanocomposites are typically prepared using synthesised or natural layered silicates. Among the different clay types, cationic layered silicate-type clay is used domestically to manufacture composites. Clay has a layered crystal structure and consists of tetrahedra, a silicon atom surrounded by four oxygen atoms, and an octahedral sheet containing metals (aluminium, iron, magnesium, and lithium) linked by eight oxygen atoms. The thickness of the clay layer is approximately 1 nm, and the lateral dimensions, ranging between 20 nm and the larger micron scale, are dependent on the class of clay and synthesis process. [36]

A variety of clays are used as reinforcing fillers, such as sepiolite, a hydrated magnesium silicate with the half-unit-cell formula $Mg_8Si_{12}O_{30}(OH)_4{\cdot}12H_2O$. It has a needle-like or fibre-like morphology comprising several blocks and tunnels oriented parallel to the fibre direction. Each structural block contains a central octahedral magnesium ($MgOH_6$) sheet sandwiched between two tetrahedral silica (SiO_4) sheets. A single sepiolite fibre is 0.2–4 µm in length, 10–30 nm in width, and 5–10 nm in thickness. [37]

Polymer–sepiolite composites have recently attracted attention because of their high aspect ratios and good thermomechanical properties. Strong interfacial bonding forces between the filler and polymer resin result in a homogeneous dispersion state. This improves the thermal and mechanical properties and introduces flame retardant properties in the composite material. [38]

A FDM 3D-printed polyethylene terephthalate glycol (PETG)–sepiolite composite was studied by Kim et al. [26]; the material showed effective synergistic mechanical reinforcement during tensile testing compared to an injection-moulded composite. The results showed that the addition of 3-phr sepiolite improved the tensile strength of the 3D-printed PETG sample by 35.4%, while the tensile strength of the injection-moulded PETG sample was improved by 7.2%.

Recently, several composite inks were developed for multifunctional applications. Graphene-based inks with improved mechanical, electrical, and organic properties can offer upgraded practicality for a wide range of 3D printing applications. [39] Jakus et al. [40] successfully fabricated a 3D printable graphene (3DG) composite, comprising graphene as the major component and polylactide-co-glycolide (PLG) as the minor component, for electronic and biomedical applications.

A basic schematic of the 3DG manufacturing process is shown in Figure 5.12. PLG and graphene powder are blended in dichloromethane (DCM), an extremely volatile solvent. During extrusion, the fast evaporation of DCM guarantees the formation of self-supporting filaments that would not distort after deposition. Subsequently, based on the user design of the 3D model, the ink is stacked into a 3D Bio Plotter (Envision TEC GmbH, Germany) to obtain a final scaffolding structure for the different applications. By proficiently evaporating the solvent, a high graphene stacking volume of 60% can be achieved using this technique. [40]

The utilisation of nanocellulose in 3D printing provides new developmental opportunities. The gel-forming properties of nanocellulose at low concentrations and its shear thinning behaviour combined with its biocompatibility, non-toxicity, and excellent mechanical properties are considered ideal for the 3D printing of nano-cellulosic implants, tissue designing materials, wound dressing materials, etc., where exact control of pore structure and geometry/shape is favourable. [41]

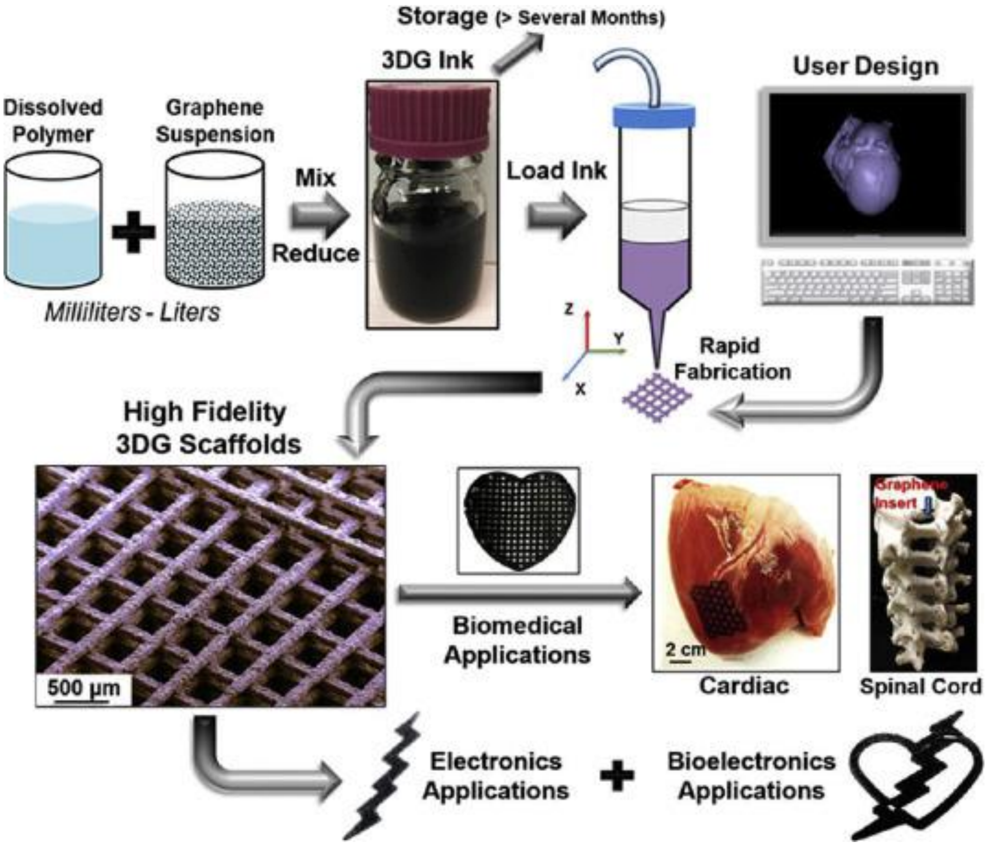

FIGURE 5.12
Fabrication of the 3DG (3D printable graphene) inks by mixing a graphene suspension with a PLG (polylactide-co-glycolide) polymer solution in a graded solvent followed by volume reduction and thickening. [40] Reproduced with permission. Copyright 2015, American Chemical Society.

Novel ceramic materials for 3D printing by photopolymerisation are composed of alumina, hydroxyapatite, zirconia, silica, etc., and distributed within a monomer matrix that is disintegrated after printing by heating at a high temperature, as reported by Doreau et al. [41], Zeng et al. [42], He et al. [43], Griffith and Halloran [44], and Felzmann et al. [45] These photopolymerisation-based printing methods are reduced forms of conventional colloidal processing of ceramics, i.e., photopolymerised tape casting and gel casting. [45] By treating these types of inks, Halloran [46] produced alumina structures with very complex shapes using DLP printing. Felzmann et al. [45] fabricated cellular Bioglass, which is used for bone repair. Other examples of DLP printing of ceramics include reports by Chabok et al. [47] and Chen et al. [48] who investigated the fabrication of piezoelectric ceramics and composites, respectively. Recently, the use of fibre-reinforced plastics (FRPs) in 3D printing have gained interest as a possible method to increase the mechanical strength and elasticity of the manufactured parts [49], [50]. The strength of these composites correspond to that of metals, but at a much lighter weight. In particular, the addition of carbon fibres to plastic resins is widely applied to improve the mechanical properties of 3D printed parts.

Nanocomposite preparation for 3D printing

Different 3D printing methods have been developed to prepare nanocomposites. These methods vary depending on the nature of the nanofiller and the resin. The main objective is to achieve a homogeneous mixture with an adequate viscosity to obtain high-quality printed products. Shear mixing, mechanical mixing, sonication, ultrasonication, or a combination of these methods may attain homogeneity.

Thermoplastics are the most commonly used materials for 3D printing, as they can be melted and reformed into the envisioned shape. While these materials have been extensively used in the fabrication of prototypes, they characteristically lack the chemical, mechanical, and thermal stability required for use in functional or load-bearing components for industrial applications. [51] Therefore, the incorporation of nanomaterials into thermoplastics to increase their thermal, chemical, and mechanical properties have gained interest .

Ning et al. [52] used the FDM process to create functional parts using carbon fibre-reinforced materials as feedstock. The type of plastic resin used heavily influenced the mechanical strength of the final product, as well as the length and loading of the carbon fibres. Carbon fibres (150 µm/100 µm) were used as reinforcing materials to improve the mechanical strength of ABS thermoplastics. The resulting composite, containing 5 wt% carbon fibres, showed a >20% increase in the Young's modulus and tensile strength of the material compared to the original ABS thermoplastic. Similarly, Yi et al. [53] used selective laser sintering (SLS) to develop and fabricate carbon/carbon (C/C) composite components, which achieved high precision and good mechanical performance. Carbon nanomaterials, such as graphene and carbon nanotubes, have unique physical and chemical properties that can improve the tensile properties and thermal stability of plastic materials. [54]

An investigation into polyurethane/poly(lactic acid)/graphene oxide nanocomposites (TPU/PLA/GO) by Chen et al. [20] showed that the addition of GO nanofillers to a TPU and PLA nanocomposite improved its mechanical properties and thermal stability. In addition, the mechanical behaviour of the TPU/PLA/GO nanocomposite is strongly dependent on its printing orientation. Additionally, they reported that the 3D printed nanocomposite exhibits good biocompatibility with NIH_3T_3 cells, showing potential as a biomaterial scaffold for tissue engineering applications.

Dul et al. [54] studied graphene nanoplatelets/acrylonitrile butadiene styrene composites. A nanofiller containing 4-wt% graphene nanoplatelets was introduced into the ABS matrix by melt blending. The results showed that the addition of graphene nanoplatelets increased the elastic modulus of pure ABS by nearly 30%. In addition to the improved elastic modulus, the graphene nanoplatelets improved the thermal stability by improving the coefficient of thermal expansion and creep compliance. Similarly, Zhuang et al. [55] studied graphene-doped polylactic acid/polylactic acid (G-PLA/PLA) composites by using pure PLA and graphene-doped polylactic acid (G-PLA) as filament materials in the dual-head printing method. The results showed that by controlling the printing parameters, the ratio of PLA to G-PLA could be varied; a higher content of G-PLA reduced the electrical resistance of the thermoplastic composites.

Torrado et al. [56] studied titanium oxide/acrylonitrile butadiene styrene composites and examined the effect of compounding 5 wt% titanium dioxide (TiO_2) nanoparticles with ABS. The results showed that there was no significant difference observed in the tensile strength of the pure ABS printed component (16.23 ± 3.07 MPa) compared to that of the ABS/TiO_2 printed component (16.22 ± 3.53 MPa). The addition of TiO_2 nanoparticles improved the tensile strength of the composite, however, varying the TiO_2 filler size slightly affected its properties. Functionalization with TiO_2 before melt blending decreased agglomeration and enriched the particle distribution in the polymer matrix. [56]

FDM printing of nanomaterials using polybutylene terephthalate (PBT) reinforced with fillers (multi-walled carbon nanotubes and graphene), was reported by Gnanasekaran et al. [57] The results showed that the 3D printed PBT/CNT composites exhibited better conductive properties, elastic behaviour, and printability than the PBT/graphene printed composites. This is because void formation during printing led to brittleness and surface roughness for the PBT/graphene 3D printed composites.

Guo et al. [58] studied cloisite/polylactic acid composites and developed a flame-retardant thermoplastic composite by using a Cloisite 30B (C-30B) nanoclay filler and PLA with melamine polyphosphate (MPP) as a matrix. The nanocomposites were prepared by melt blending and then treated as filaments using a single screw extruder. The PLA/MPP polymer composites showed poor heat conduction, resulting in flame resistivity and significantly decreased mechanical properties. However, the addition of the C-30B nanoclay fillers improved the mechanical properties of the thermoplastic nanocomposites. The modulus and tensile strength of the 3D printed PLA/MPP/C30B nanocomposites were 3.91 ± 0.22 GPa and 70.0 ± 3.8 MPa, respectively.

Rheological properties of nanocomposites

To determine the printability of nanocomposites, it is important to determine the behaviour of the material when it passes through the nozzle, and thus the rheological properties of the molten material. Rheology is an active and suitable indicator of the flow properties of fresh composites. The use of rheological models is recognised as an efficient tool to predict the fresh properties of composites.

Different nanomaterials have been added to polymers to improve their properties in the hardened state. The nanomaterials exhibit a high specific surface area to volume ratio, which makes them highly reactive during hydration. [59] The higher surface areas of nanomaterials increase their water requirements within the mixture, which may result in the scarcity of dispersed water in an aqueous system. Nanomaterials in polymer materials may act as filler particles that densify the microstructure of the composite, thus decreasing the porosity of the hardened polymer. [59]

Nanosilica is a vastly active pozzolanic material containing glassy particles approximately 1000 times smaller than the corresponding polymer materials. [60], [61] Nanosilica influences the hydration kinetics of the composite material owing to its high specific surface area, which in turn develops the microstructure of the material and promotes its pozzolanic activity. Nanosilica can react with $Ca(OH)_2$ and act as nucleation sites for the formation of calcium-silicate-hydrate (CSH) gels. [62], [63] However, it is still unclear whether the increase in the hydration process is due to the higher specific surface area of the CSH gel or its chemical reactivity. [64] A significant improvement in the hydration process and a reduction in the setting time and formation of calcium-silicate-hydrate (CSH) gel was observed after 9 h of mixing. [65] Senff et al. [66] used a factorial design approach with a rheometer and flow table test to study the collective effect of nanosilica and nanotitania on the flow properties of mortars. They presented the most effective combination of both nanomaterials along with the proportion of super plasticizer required to achieve significant rheology with compressive strength.

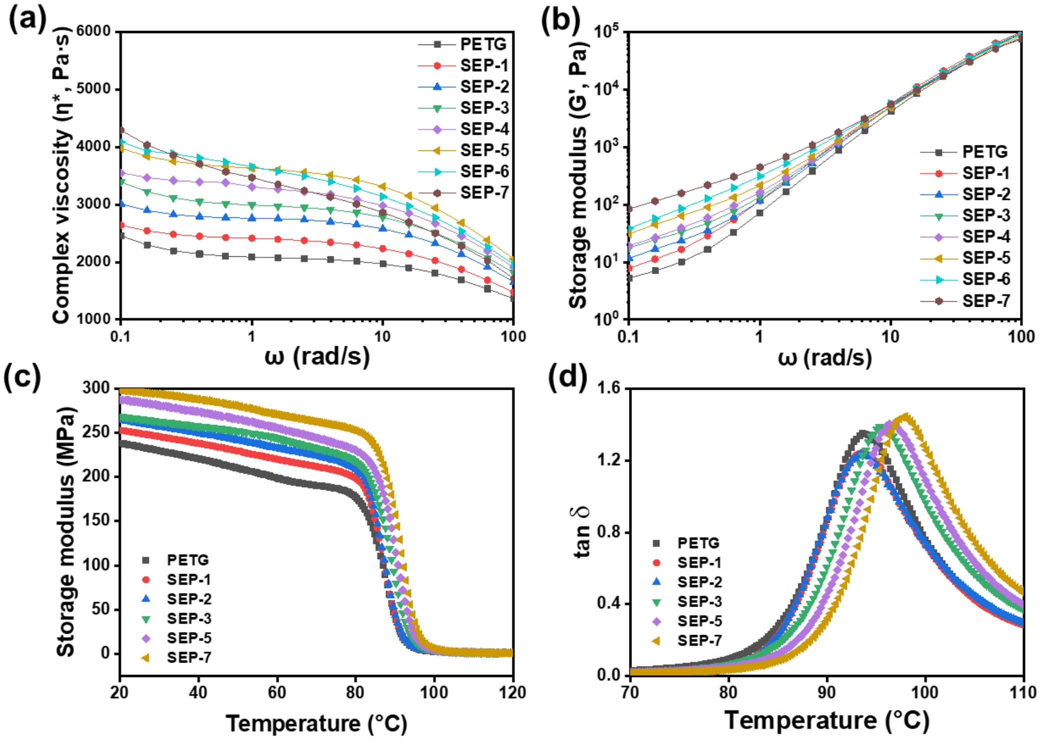

FIGURE 5.13
Rheological characterization of the PETG and PETG-SEP composite materials. The (a) complex viscosity *η** and (b) storage modulus *G′* with frequency *ω* curves for the pure PETG and PETG-SEP nanocomposites in the molten state at 200 °C. Temperature dependencies of the (e) storage modulus *G′* and (f) tan δ (ratio of loss modulus to storage modulus) of pure PETG and the PETG-SEP nanocomposites. [26] Reproduced with permission. Copyright 2020, American Chemical Society.

Bagheriasl et al. (2016) reported the preparation of a polymer-cellulose nanocrystal (CNC) nanocomposite, which showed good dispersion of the CNCs within the polylactide (PLA) matrix, consequently resulting in the lowest rheological percolation threshold reported thus far for polymer-CNC systems. The rheological behaviours of the nanocomposites were determined in dynamic, transient, and steady-shear flow fields in the molten state. The complex viscosity and storage modulus of the nanocomposites increased markedly with the CNC content, particularly at low frequencies; the samples exhibited high shear thinning and a transition from liquid- to solid-like behaviour with an increase in the CNC concentration. [67]

Kumar et al. (2012) showed that the combination of photocurable resins and CNCs demonstrated rheological properties of composite materials. The changes in storage modulus (G′) and loss modulus (G″) of the CNC/stereolithography resin (SLR) mixture as a function of frequency and CNC content were shown. Both G′ and G″ of the neat resin increased with increasing frequency in an essentially linear fashion. Both moduli also increased upon the introduction of CNCs. The frequency dependence of G′ and G″ was dampened upon the introduction of the CNCs, i.e., the slopes of the G′ and G″ vs frequency curves eventually decreased compared to those of the neat resin. This difference is most pronounced when using ≥ 1.0% w/w CNCs in the case of G′ and ≥ 5.0% w/w CNCs in the case of G″, suggesting a transition from a liquid-like to solid-like state. [68]

To comprehend the state of a PETG-sepiolite composite filament as it passes through the nozzle during 3D printing, the rheological properties of the molten polymeric material is required. The rheological behaviour affects the processability and structure-processing relationship of the material. A sepiolite concentration of ≥1 phr affects the rheological properties of PETG, and at 7 phr, the complex viscosity and storage modulus show an approximate two-fold increase compared to those of pure PETG. The good dispersion of sepiolite in PETG results in network formation and the transition from liquid- to solid-like behaviour. [26]

Mechanical properties of printed composite materials

All 3D printing material (We have to write the content). Carneiro et al. (2015) studied the potential of PP as a candidate for FDM-based 3D printing techniques. The entire filament production chain was evaluated, starting with the PP pellets, filament production by extrusion, and test sample printing. This strategy enables a true comparison between the components printed and the components manufactured by compression moulding using the same grade of raw material. The printed samples were mechanically characterised, and the influence of filament orientation, layer thickness, infill degree, and material was assessed. Regarding the latter, two grades of PP were evaluated: glass-fibre-reinforced PP and neat non-reinforced PP. The results showed the potential of FDM to compete with conventional techniques, especially for the production of a small series of parts/components. In addition, this technique produces components with adequate mechanical performance and, therefore, does not need to be restricted to the production of mock-ups and prototypes. [12]

Weng et al. (2016) reported the preparation of ABS nanocomposites containing organic-modified montmorillonite (OMMT) by melt intercalation. ABS nanocomposite filaments for FDM 3D printing were produced using a single screw extruder and printed using a commercial FDM 3D printer. The 3D printed samples were evaluated by tensile, flexural, thermal expansion, and dynamic mechanical tests. The structures of the nanocomposites were analysed using TEM and low-angle XRD. The results showed that the addition of 5 wt% OMMT improved the tensile strengths of the 3D printed ABS samples by 43%, while the tensile strengths of the injection moulded ABS samples were improved by 28.9%. It was established that the addition of OMMT significantly increased the tensile modulus, flexural strength, flexural modulus, and dynamic mechanical storage modulus, and decreased the linear thermal expansion ratio and weight loss determined by TGA. These novel ABS nanocomposites, exhibiting good mechanical and thermal properties, are promising materials for FDM 3D printing. [69]

Organically modified nanofillers, including nano SiO_2, montmorillonite, and attapulgite, were loaded onto SLR. The surfaces of the nanofillers were modified using organic modifiers, 3-(trimethoxysilyl)propyl methacrylate (γ-MPS) and (1-hexadecyl)dimethyl allyl ammonium chloride (C16-DMAAC), and characterised by FTIR and low-angle XRD analysis. The morphologies of the nanocomposites were observed using TEM. The viscosities and curing speeds of the SLR nanocomposites containing increasing nanofiller loadings were also studied. Furthermore, the mechanical properties of the printed samples fabricated using an in-house SLA 3D printer, were tested. The influence of the nanoparticles on the printing accuracy was also measured and discussed. It was established that the addition of 5% w/w nano SiO_2 increased the tensile strength and modulus of the composite by 20.6% and 65.1%, respectively, and this did not significantly influence the printed accuracy. [70] Thus, blending a nanomaterial and a photocurable resin in the form of a composite material, significantly affects the curing behaviour of the material and its properties after curing.

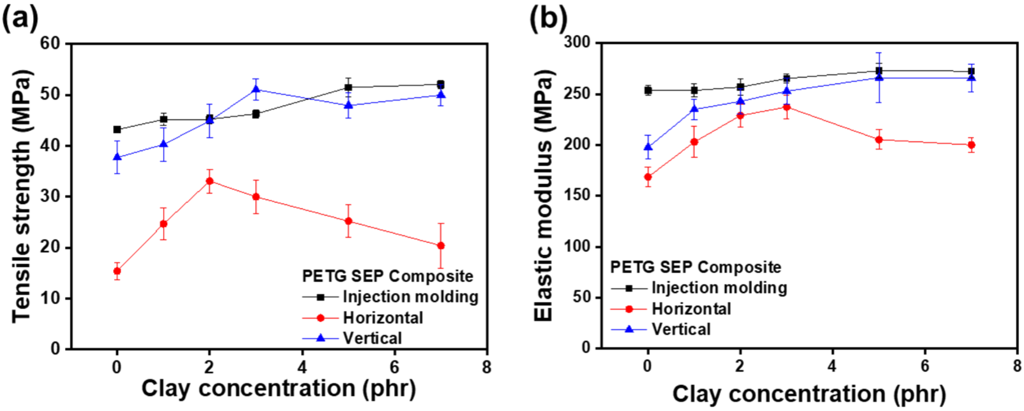

FIGURE 5.14
Change in the tensile strength characteristics based on the 3D printing direction. Measurements of the mechanical properties of the PETG nanocomposites containing varying SEP concentrations: (a) tensile strength and (b) Young's modulus. [26] Reproduced with permission. Copyright 2020, American Chemical Society.

The most recent reports indicate that FDM 3D printed PETG-sepiolitic composites show effective synergistic mechanical strengthening during tensile tests compared to injection-moulded composites. As a result, the addition of 3 phr sepiolite improved the tensile strength of the 3D printed PETG sample by 35.4%, while the tensile strength of the injection-moulded PETG sample was improved by 7.2%. These micro-oriented nanostructures which formed during 3D printing created a synergistic effect that improved the material properties of the composite. Taking into account its improved mechanical properties, this new PETG-sepiolite composite could be a promising FDM 3D printed material. [26] Thus, nanomaterials show excellent mechanical strength reinforcement when applied to 3D printing.

3D printing materials for the biomedical field

3D printing has been applied in several fields, including the automotive industry, electronics, airplane engines, and architecture. In particular, there are advantages to applying 3D printing technology in the medical field [71], such as its customisability which is essential to achieve components that have patient-specific shapes and mechanical strengths. The traditional method involves high production costs and extended production times, and it is difficult to properly match the area with bone contours; therefore, hand forming is performed through manual bending. 3D printing technology could overcome these drawbacks of the traditional methods. [72]

3D printing technology can produce precise geometries using data obtained from medical imaging of the patient; thus, a more accurate design is possible through fitting test matching between the implant to be inserted and the part of the patient's body that was printed. [72] In addition, 3D printing technology helps doctors perform surgical planning and simulation to enable improved surgery, and facilitates the manufacture of permanent and temporary dental components. As shown in Figure 5.15, AM has been applied in several medical fields, including regenerative medicine, implants, cardiology, orthopaedics, and dentistry. [71], [73–75]

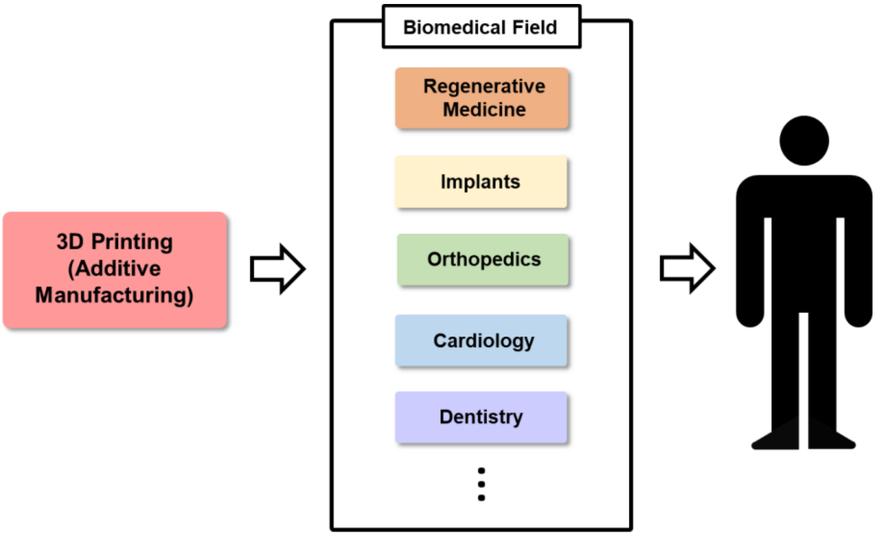

FIGURE 5.15
Additive manufacturing application within biomedical field. [71]

The essential factors to consider for 3D printed medical materials are printability, structural and mechanical properties, degradation kinetics, by-products, and biocompatibility. First, the materials used in 3D printing of medical components must have viscosity and rheological properties that facilitate handling and deposition. Subsequently, spatial and temporal control makes precise construction possible. [76] Specifically, when inkjet printing biomaterials, a phase transition from sol to gel should be possible after ejection from the print head. The ideal materials to extrude through the nozzle are shear-thinning and non-Newtonian materials. If a shear-thickening fluid is used, the nozzle could be clogged, and the thixotropic fluid, exhibiting viscosity as a function of time, may result in inhomogeneous structures. [77] In addition, low-viscosity resins or high molecular weight resins diluted with large amounts of monomer should be used in photo-curing-based printing, such as DLP or SLA. [75]

Second, for the 3D structure to maintain its structural properties, it should have mechanical properties that are sufficient to resist external forces. Depending on the tissue type, ranging from skin and liver to bone, the required mechanical properties of the structure vary. Therefore, the materials need to be carefully selected according to the required mechanical properties. [76] For example, scaffolds for cortical bones should have a compressive strength of 100 MPa, while those for spongy bones should have a compressive strength of 3.9 MPa. Thus, different mechanical properties are required depending on the location and type of material to be applied. [77]

Third, ideally, the rate of biodegradability should match the rate at which the material is replaced with new tissue, however, this is challenging. Each material has a different biodegradation rate in vivo; therefore, it is necessary to carefully select the material before use. In addition, the degradation by-product is an important factor; it should be non-toxic, readily metabolised, and rapidly cleared from the body. Toxic by-products have a fatal effect on cell viability and function.

Notably, although large molecular weight polymers are initially inert, they break down into monomers or oligomers. This can cause inflammation and other fatal adverse effects. [76]
Fourth, biocompatibility has traditionally been associated with the use of implantable devices. It is regarded as an instrument that will remain for a long time and cause the lowest number of chemical reactions in the human body. Therefore, material selection is based on the following criteria: It should be non-toxic, non-immunogenic, non-thrombogenic, non-carcinogenic, non-irritant, etc. However, the concept of biocompatibility has evolved over time. The specific requirements could alter not only the characteristics of the material itself, but also the application site and situation. In some cases, the materials are required to specifically react with the tissue rather than be completely inert. In addition, some materials are required to be biodegradable in the body over time. [78]

Biocompatible 3D printing materials and composites

As mentioned in the previous section, the material characteristics for application in the biomedical field are quite complex. Ceramic and polymer materials that satisfy these criteria are used as biocompatible materials.

Ceramics

Ceramics, as biomaterials, contain metals and inorganic calcium and phosphate salts. As calcium and phosphate salts mimic the inorganic content of bone tissue, these materials can be used as biomaterials. [77] Calcium phosphate can chemically bond to body tissue and is relatively soluble. In addition, calcium phosphate, as a metabolite ion, can participate in calcium and phosphorous circulation in the human body and is not harmful. [79] These bioresorbable materials are applicable because they have natural osteoconductive (promotes new bone growth) and osteoinductive (promotes cell differentiation towards osteoblastic lineage without using growth factors) properties. [77]
Based on literature reports, ceramic biomaterials used for 3D printing include calcium sulphate [80], hydroxyapatite [79], [81], biphasic calcium phosphate (BCP) [79], [82], CPC (mixture of α-tricalcium phosphate (α-TCP) and calcium-deficient HA) [83], and β-TCP [84]. Although ceramic biomaterials exhibit excellent biocompatibility, they are extremely difficult to process because of the extreme hardness and brittleness of the ceramic components. This can not only cause serious wear of the processing equipment, but can also cause defects, such as cracking, in the ceramic sections; thus, it is difficult to achieve good surface quality. [85] To improve this, studies have been conducted in which ceramics and polymers, including ε-polycaprolactone (PCL), PLA, poly L-lactide-glycolic acid (PLGA), polyethylene glycol diacrylate (PEGDA), Alginate, etc., are mixed to form composites.

Polymers

PLA, PLGA, PCL, and PEGDA are the most commonly used biocompatible materials in 3D printing. Among them, PLA is the most widely used biodegradable polymer as it has the advantage of high modulus, excellent biocompatibility and is approved by the US Food and Drug Administration (FDA); however, it also has the disadvantages of low elongation and brittleness, low cell adhesion, proliferation, and differentiation in biological systems. [86] To improve its biological properties, it is blended with other polymers [87], synthesised as copolymers [88], and combined with ceramics to be applied in tissue engineering [82], [86].

PLGA is a copolymer of PLA that exhibits excellent biocompatibility and has been approved by the FDA. Notably, PLGA has a faster biodegradation rate of approximately 1–6 weeks in physiological conditions compared to PLA which has a biodegradation rate of approximately 11–18 weeks. The biodegradation rate and mechanical properties of PLGA can be adjusted by changing the glycolic acid to lactic acid copolymer ratio. With an increase in the lactic acid content, the hydrophilic properties decrease, inhibiting water penetration and the biodegradation rate. [89] As the required physical properties and biodegradation rates vary according to tissue, it is advantageous that the properties of PLGA can be easily controlled. However, it has recently been reported that PLA and its copolymer can cause inflammatory reactions when they decompose in vivo. Fortunately, this phenomenon is localised close to the implanted material and is not systemic. This suggests that appropriate toxicology, biocompatibility, and biodegradability studies should be performed before these materials are used in applications as they could react differently in different tissues. [90]

PCL exhibits unique thermal properties. The melting temperature of PCL is 59–64 °C, its T_g is approximately -60 °C, and it exhibits a rubbery state at physiological temperature. As a result, PCL has high toughness, which can be used to reinforce the mechanical properties of other polymers. The degradation time of PCL under physiological conditions is approximately 2–3 years slower than that of PLA and PLGA, because it contains more hydrophobic $-CH_2$ moieties in its repeating unit. It is also non-toxic and biocompatible and is used in regenerative therapy and drug delivery applications. [91]

PEGDA can be modified to a crosslinkable polymer by replacing the terminal hydroxyl group of the PEG unit with acrylate. PEG also has excellent biocompatibility according to the FDA, however, it cannot withstand the shear force generated by joints owing to its low strength and ductility. Substituting PEG with PEGDA, solves this problem. PEGDA can also be used in photo-curing 3D printing, enabling more precise and fast printing. [92] However, the photo-curing resin material is mostly cytotoxic owing to the unreacted double bond in the photosensitive resin and residual photoinitiator. Photo-cured 3D printed materials have been mainly used in the dental field for indirect or transient contact with the living body. [75]

Biocompatible nanomaterials for 3D printing

Nanomaterials are applied in several applications as a small amount can considerably increase desirable properties. Studies have been conducted to improve the mechanical properties and biochemical functions of materials used in the medical field by the introduction of nanomaterials.

Graphene, an allotrope of carbon composed of sp2 hybridized carbon atoms arranged in a 2D honeycomb lattice, is frequently used as a biocompatible nanomaterial. It has drawn attention in bone regenerative engineering as its unique structure can improve the mechanical strength of the biomaterial and promote cell adhesion and growth. As indicated in Figure 5.16, graphene-based biomaterials can provide positive reinforcing (strength, stiffness, and toughness) and biological effects when used in regenerative engineering. Thus, research on graphene-based biocompatible 3D printing materials is continuously increasing. [93]

The addition of nano-sized materials to ceramics, materials that exhibit complimentary properties with the incorporation of polymers, can yield significantly meaningful results. Deng et al.[93] reported remarkable mechanical strength and biocompatibility results by incorporating nano-hydroxyapatite (n-HA) into PEGDA through in situ photopolymerisation. The compressive strength and compression modulus increased by 342% and 215%, respectively, compared to those of neat PEGDA. These properties are critical for the material to function as a scaffold. In addition, the wettability and cell viability significantly increased with the addition of n-HA. [92]

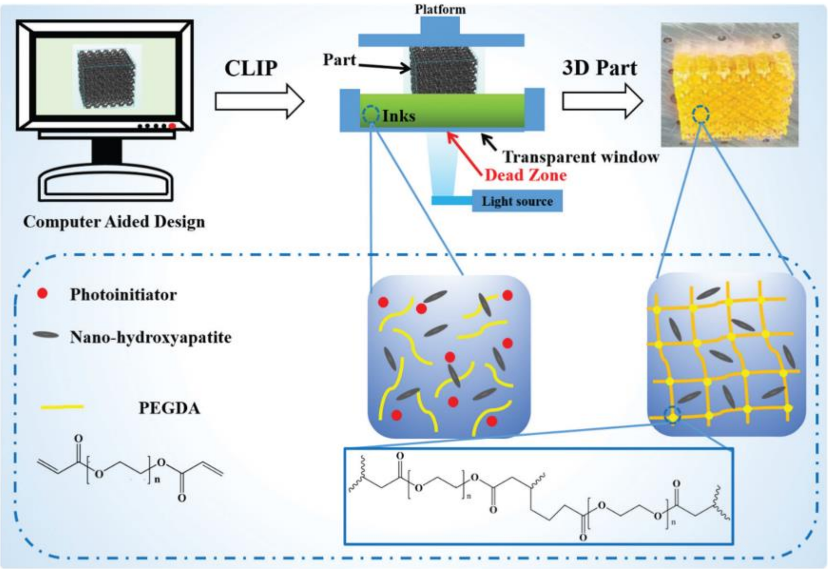

FIGURE 5.16
The working process followed for the formation of the scaffold and the reaction mechanism of the n-HA/PEGDA ink under light radiation. [92] Reproduced with permission. Copyright 2021, the royal society of chemistry.

Nanocellulose, including CNCs and cellulose nanofibres (CNFs), can be applied to 3D printing hydrogels as biocompatible nanomaterials. Hydrogels are widely used to replace the extracellular matrix (ECM) in 3D printing tissue engineering. Hydrogels are hydrated polymeric materials containing more than 90% water; examples include collagen, gelatine, pullulan, hyaluronic acid, PLGA, PEG, PCL, and polyethylene oxide (PEO). Unfortunately, owing to its low mechanical strength and poor crosslinking, hydrogels cannot support the structural shape of 3D printed materials or achieve high resolution. To improve the limitations of hydrogels, nanocellulose, such as CNCs and CNFs, can be incorporated. These composites containing nanocellulose exhibit the following characteristics: (1) improved viscoelasticity, (2) preserved printed complex macrostructure for cellular proliferation, (3) large surface area, and (4) small volumetric shrinkage. The composites are also biocompatible, biodegradable, non-toxic, and contains an abundance of hydroxyl groups. The large surface area of nanocellulose allows for enhanced tissue formation. Therefore, it has been applied in cell scaffolds, tissue engineering, and wound dressings. [94], [95]

To date, several studies on biocompatible materials applicable to 3D printing have been reported. 3D printing technology for medical applications should continue to attract attention, considering its advantages which include, patient customisation, material selection based on mechanical properties and biodegradability, and cost.

Conclusions

In this chapter, we discussed the application of nanomaterials in 3D printing. There are several electrical, mechanical, and biological property advantages, which have been extensively studied, to the application of nanocomposite material technology to 3D printing. Mechanical strength, such as tensile and modulus strength, increases with the incorporation of nanomaterials to conventional 3D printing materials, and electrical conductivity can be imparted by using conductive nanomaterials. Bone can be replaced by materials that exhibit high biological engraftment and bone cement properties. In addition, we investigated the changes in the rheological behaviour of polymers and resins with the incorporation of nanomaterials. Understanding these rheological behaviours can facilitate the application of nanocomposites to 3D printing. We also presented preparation methods for various nanocomposite materials for 3D printing. In conclusion, the use of nanomaterials in 3D printing technology unlocks several possibilities for future applications.

References

1. Ngo, T. D., Kashani, A., Imbalzano, G., Nguyen, K. T. Q. & Hui, D. Additive manufacturing (3D printing): A review of materials, methods, applications and challenges. *Composites Part B: Engineering* vol. 143 172–196 (2018).
2. Página de detalle del comunicado de prensa | TRUMPF. https://www.trumpf.com/es_INT/empresa/presse/comunicados-de-prensa-mundial/pagina-de-detalle-del-comunicado-de-prensa-global/Press/emo-hannover-2019-trumpf-is-expanding-the-scope-of-3d-printing/.
3. Berman, B. 3-D printing: The new industrial revolution. *Bus. Horiz.* **55**, 155–162 (2012).
4. Yan, C., Jiang, P., Jia, X. & Wang, X. 3D printing of bioinspired textured surfaces with superamphiphobicity. *Nanoscale* vol. 12 2924–2938 (2020).
5. Campbell, T. A. & Ivanova, O. S. 3D printing of multifunctional nanocomposites. *Nano Today* **8**, 119–120 (2013).
6. Prashantha, K. & Roger, F. Multifunctional properties of 3D printed poly(lactic acid)/graphene nanocomposites by fused deposition modeling. *J. Macromol. Sci. Part A* **54**, 24–29 (2017).
7. Kumar, N. & Sinha Ray, S. Synthesis and functionalization of nanomaterials. in *Springer Series in Materials Science* vol. 277 15–55 (Springer Verlag, 2018).
8. Mohamed, O. A., Masood, S. H. & Bhowmik, J. L. Optimization of fused deposition modeling process parameters: a review of current research and future prospects. *Adv. Manuf.* **3**, 42–53 (2015).
9. Waheed, S. *et al.* 3D printed microfluidic devices: Enablers and barriers. *Lab on a Chip* vol. 16 1993–2013 (2016).
10. Yin, J., Lu, C., Fu, J., Huang, Y. & Zheng, Y. Interfacial bonding during multi-material fused deposition modeling (FDM) process due to inter-molecular diffusion. *Mater. Des.* **150**, 104–112 (2018).
11. Tian, X., Liu, T., Yang, C., Wang, Q. & Li, D. Interface and performance of 3D printed continuous carbon fiber reinforced PLA composites. *Compos. Part A Appl. Sci. Manuf.* **88**, 198–205 (2016).

12. Carneiro, O. S., Silva, A. F. & Gomes, R. Fused deposition modeling with polypropylene. *Mater. Des.* **83**, 768–776 (2015).
13. Melchels, F. P. W., Feijen, J. & Grijpma, D. W. A review on stereolithography and its applications in biomedical engineering. *Biomaterials* vol. 31 6121–6130 (2010).
14. Andrzejewska, E. Photopolymerization kinetics of multifunctional monomers. *Progress in Polymer Science (Oxford)* vol. 26 605–665 (2001).
15. Bhattacharjee, N., Urrios, A., Kang, S. & Folch, A. The upcoming 3D-printing revolution in microfluidics. *Lab on a Chip* vol. 16 1720–1742 (2016).
16. Regehly, M. *et al.* Xolography for linear volumetric 3D printing. *Nature* **588**, 620–624 (2020).
17. Le Duigou, A., Barbé, A., Guillou, E. & Castro, M. 3D printing of continuous flax fibre reinforced biocomposites for structural applications. *Mater. Des.* **180**, 107884 (2019).
18. Jordan, R. S. & Wang, Y. 3D printing of conjugated polymers. *J. Polym. Sci. Part B Polym. Phys.* **57**, 1592–1605 (2019).
19. Wojtyła, S., Klama, P. & Baran, T. Is 3D printing safe? Analysis of the thermal treatment of thermoplastics: ABS, PLA, PET, and nylon. *J. Occup. Environ. Hyg.* **14**, D80–D85 (2017).
20. Chen, Q. *et al.* 3D printing biocompatible polyurethane/poly(lactic acid)/graphene oxide nanocomposites: Anisotropic properties. *ACS Appl. Mater. Interfaces* **9**, 4015–4023 (2017).
21. Eerkes-Medrano, D., Leslie, H. A. & Quinn, B. Microplastics in drinking water: A review and assessment. *Current Opinion in Environmental Science and Health* vol. 7 69–75 (2019).
22. Panno, S. V. *et al.* Microplastic Contamination in Karst Groundwater Systems. *Groundwater* **57**, 189–196 (2019).
23. Wang, Y. *et al.* Effects of ingested polystyrene microplastics on brine shrimp, Artemia parthenogenetica. *Environ. Pollut.* **244**, 715–722 (2019).
24. Karami, A. *et al.* The presence of microplastics in commercial salts from different countries. *Sci. Rep.* **7**, 1–11 (2017).
25. Kim, S. W. & An, Y. J. Soil microplastics inhibit the movement of springtail species. *Environ. Int.* **126**, 699–706 (2019).
26. Kim, H. *et al.* 3D Printing of Polyethylene Terephthalate Glycol-Sepiolite Composites with Nanoscale Orientation. *ACS Appl. Mater. Interfaces* **12**, 23453–23463 (2020).
27. Dawoud, M., Taha, I. & Ebeid, S. J. Mechanical behaviour of ABS: An experimental study using FDM and injection moulding techniques. *J. Manuf. Process.* **21**, 39–45 (2016).
28. Serra, T., Planell, J. A. & Navarro, M. High-resolution PLA-based composite scaffolds via 3-D printing technology. *Acta Biomater.* **9**, 5521–5530 (2013).
29. Fu, J. *et al.* Combination of 3D printing technologies and compressed tablets for preparation of riboflavin floating tablet-in-device (TiD) systems. *Int. J. Pharm.* **549**, 370–379 (2018).
30. Bagheri, A. & Jin, J. Photopolymerization in 3D Printing. *ACS Appl. Polym. Mater.* **1**, 593–611 (2019).
31. Ahmed Khan, T., Zakaria, M. E. T., Kim, H., Ghazali, S. & Jamari, S. S. Carbonaceous microsphere-based superabsorbent polymer as filler for coating of NPK fertilizer: Fabrication, properties, swelling, and nitrogen release characteristics. *J. Appl. Polym. Sci.* **137**, 48396 (2020).
32. Khan, T. A. *et al.* Hydrothermal carbonization of lignocellulosic biomass for carbon rich material preparation: A review. *Biomass and Bioenergy* vol. 130 105384 (2019).

33. Ahmed Khan, T., Kim, H. J., Gupta, A., Jamari, S. S. & Jose, R. Synthesis and characterization of carbon microspheres from rubber wood by hydrothermal carbonization. *J. Chem. Technol. Biotechnol.* **94**, 1374–1383 (2019).
34. Kim, H., Park, J.-W. & Kim, H.-J. Flame Retardant Nano-Composites containing Nano-Fillers. in *Science and applications of Tailored Nanostructures* (ed. Paolo, D. S.) 1–28 (onecentralpress, 2017).
35. Bukkapatnam, S., Kamarthi, S., Huang, Q., Zeid, A. & Komanduri, R. Nanomanufacturing systems: Opportunities for industrial engineers. *IIE Trans. (Institute Ind. Eng.* **44**, 492–495 (2012).
36. Sinha Ray, S. & Okamoto, M. Polymer/layered silicate nanocomposites: A review from preparation to processing. *Progress in Polymer Science (Oxford)* vol. 28 1539–1641 (2003).
37. Tabatabaei-Yazdi, Z. & Mehdipour-Ataei, S. Poly(ether-imide) and related sepiolite nanocomposites: investigation of physical, thermal, and mechanical properties. *Polym. Adv. Technol.* **26**, 308–314 (2015).
38. Kim, H. *et al.* Clay-organic intumescent hybrid system for the synergetic flammability of polymer nanocomposites. *J. Therm. Anal. Calorim.* **132**, 2009–2014 (2018).
39. Torrisi, F. & Coleman, J. N. Electrifying inks with 2D materials. *Nat. Nanotechnol.* **9**, 738–739 (2014).
40. Jakus, A. E. *et al.* Three-dimensional printing of high-content graphene scaffolds for electronic and biomedical applications. *ACS Nano* **9**, 4636–4648 (2015).
41. Sultan, S., Siqueira, G., Zimmermann, T. & Mathew, A. P. 3D printing of nano-cellulosic biomaterials for medical applications. *Current Opinion in Biomedical Engineering* vol. 2 29–34 (2017).
42. Zeng, Y. *et al.* 3D printing of hydroxyapatite scaffolds with good mechanical and biocompatible properties by digital light processing. *J. Mater. Sci.* **53**, 6291–6301 (2018).
43. He, R. *et al.* Fabrication of complex-shaped zirconia ceramic parts via a DLP-stereolithography-based 3D printing method. *Ceram. Int.* **44**, 3412–3416 (2018).
44. Griffith, M. L. & Halloran, J. W. Freeform Fabrication of Ceramics via Stereolithography. *J. Am. Ceram. Soc.* **79**, 2601–2608 (2005).
45. Felzmann, R. *et al.* Lithography-Based Additive Manufacturing of Cellular Ceramic Structures. *Adv. Eng. Mater.* **14**, 1052–1058 (2012).
46. Halloran, J. W. Ceramic Stereolithography: Additive Manufacturing for Ceramics by Photopolymerization. *Annu. Rev. Mater. Res.* **46**, 19–40 (2016).
47. Chabok, H. *et al.* Ultrasound transducer array fabrication based on additive manufacturing of piezocomposites. in *ASME/ISCIE 2012 International Symposium on Flexible Automation, ISFA 2012* 433–444 (American Society of Mechanical Engineers (ASME), 2012). doi:10.1115/ISFA2012-7119.
48. Chen, Z. *et al.* 3D printing of piezoelectric element for energy focusing and ultrasonic sensing. *Nano Energy* **27**, 78–86 (2016).
49. Nikzad, M., Masood, S. H. & Sbarski, I. Thermo-mechanical properties of a highly filled polymeric composites for Fused Deposition Modeling. *Mater. Des.* **32**, 3448–3456 (2011).
50. Mallick, P. K. *Fiber-Reinforced Composites: Materials, Manufacturing, and Design*. (CRC Press, 2007).
51. Tekinalp, H. L. *et al.* Highly oriented carbon fiber-polymer composites via additive manufacturing. *Compos. Sci. Technol.* **105**, 144–150 (2014).

52. Ning, F., Cong, W., Hu, Y. & Wang, H. Additive manufacturing of carbon fiber-reinforced plastic composites using fused deposition modeling: Effects of process parameters on tensile properties. *J. Compos. Mater.* **51**, 451–462 (2017).
53. Yi, X. *et al.* Three dimensional printing of carbon/carbon composites by selective laser sintering. *Carbon* vol. 96 603–607 (2016).
54. Dul, S., Fambri, L. & Pegoretti, A. Fused deposition modelling with ABS-graphene nanocomposites. *Compos. Part A Appl. Sci. Manuf.* **85**, 181–191 (2016).
55. Zhuang, Y. *et al.* 3D–printing of materials with anisotropic heat distribution using conductive polylactic acid composites. *Mater. Des.* **126**, 135–140 (2017).
56. Torrado, A. R. *et al.* Characterizing the effect of additives to ABS on the mechanical property anisotropy of specimens fabricated by material extrusion 3D printing. *Addit. Manuf.* **6**, 16–29 (2015).
57. Gnanasekaran, K. *et al.* 3D printing of CNT- and graphene-based conductive polymer nanocomposites by fused deposition modeling. *Appl. Mater. Today* **9**, 21–28 (2017).
58. Guo, Y. *et al.* Engineering flame retardant biodegradable polymer nanocomposites and their application in 3D printing. *Polym. Degrad. Stab.* **137**, 205–215 (2017).
59. Sanchez, F. & Sobolev, K. Nanotechnology in concrete - A review. *Construction and Building Materials* vol. 24 2060–2071 (2010).
60. Lavergne, F., Belhadi, R., Carriat, J. & Ben Fraj, A. Effect of nano-silica particles on the hydration, the rheology and the strength development of a blended cement paste. *Cem. Concr. Compos.* **95**, 42–55 (2019).
61. Reches, Y. Nanoparticles as concrete additives: Review and perspectives. *Construction and Building Materials* vol. 175 483–495 (2018).
62. Balapour, M., Joshaghani, A. & Althoey, F. Nano-SiO2 contribution to mechanical, durability, fresh and microstructural characteristics of concrete: A review. *Construction and Building Materials* vol. 181 27–41 (2018).
63. Kuo, W.-T., Lin, K.-L., Chang, W.-C. & Luo, H.-L. *Effects of Nano-Materials on Properties of Waterworks Sludge Ash Cement Paste*. *J. Ind. Eng. Chem* vol. 12 https://www.cheric.org/research/tech/periodicals/view.php?seq=541371 (2006).
64. Björnström, J., Martinelli, A., Matic, A., Börjesson, L. & Panas, I. Accelerating effects of colloidal nano-silica for beneficial calcium-silicate-hydrate formation in cement. *Chem. Phys. Lett.* **392**, 242–248 (2004).
65. Senff, L., Labrincha, J. A., Ferreira, V. M., Hotza, D. & Repette, W. L. Effect of nano-silica on rheology and fresh properties of cement pastes and mortars. *Constr. Build. Mater.* **23**, 2487–2491 (2009).
66. Senff, L., Hotza, D., Lucas, S., Ferreira, V. M. & Labrincha, J. A. Effect of nano-SiO2 and nano-TiO2 addition on the rheological behavior and the hardened properties of cement mortars. *Mater. Sci. Eng. A* **532**, 354–361 (2012).
67. Bagheriasl, D., Carreau, P. J., Riedl, B., Dubois, C. & Hamad, W. Y. Shear rheology of polylactide (PLA)–cellulose nanocrystal (CNC) nanocomposites. *Cellulose* **23**, 1885–1897 (2016).
68. Kumar, S., Hofmann, M., Steinmann, B., Foster, E. J. & Weder, C. Reinforcement of stereolithographic resins for rapid prototyping with cellulose nanocrystals. *ACS Appl. Mater. Interfaces* **4**, 5399–5407 (2012).
69. Weng, Z., Wang, J., Senthil, T. & Wu, L. Mechanical and thermal properties of ABS/montmorillonite nanocomposites for fused deposition modeling 3D printing. *Mater. Des.* **102**, 276–283 (2016).

70. Weng, Z., Zhou, Y., Lin, W., Senthil, T. & Wu, L. Structure-property relationship of nano enhanced stereolithography resin for desktop SLA 3D printer. *Compos. Part A Appl. Sci. Manuf.* **88**, 234–242 (2016).
71. Nadagouda, M. N., Rastogi, V. & Ginn, M. A review on 3D printing techniques for medical applications. *Curr. Opin. Chem. Eng.* **28**, 152–157 (2020).
72. Moiduddin, K. *et al.* Structural and mechanical characterization of custom design cranial implant created using additive manufacturing. *Electron. J. Biotechnol.* **29**, 22–31 (2017).
73. Wong, T. M. *et al.* The use of three-dimensional printing technology in orthopaedic surgery: A review. *J. Orthop. Surg.* **25**, 1–7 (2017).
74. Vasamsetty, P., Pss, T., Kukkala, D., Singamshetty, M. & Gajula, S. 3D printing in dentistry - Exploring the new horizons. *Mater. Today Proc.* **26**, 838–841 (2019).
75. Quan, H. *et al.* Photo-curing 3D printing technique and its challenges. *Bioact. Mater.* **5**, 110–115 (2020).
76. Murphy, S. V. & Atala, A. 3D bioprinting of tissues and organs. *Nat. Biotechnol.* **32**, 773–785 (2014).
77. Jammalamadaka, U. & Tappa, K. Recent advances in biomaterials for 3D printing and tissue engineering. *J. Funct. Biomater.* **9**, (2018).
78. Williams, D. F. On the mechanisms of biocompatibility. *Biomaterials* **29**, 2941–2953 (2008).
79. Sun, H. *et al.* 3D printing of calcium phosphate scaffolds with controlled release of antibacterial functions for jaw bone repair. *Mater. Des.* **189**, 108540 (2020).
80. Huang, K.-H., Wang, C.-Y., Chen, C.-Y., Hsu, T.-T. & Lin, C.-P. Incorporation of Calcium Sulfate Dihydrate into a Mesoporous Calcium Silicate/Poly-ε-Caprolactone Scaffold to Regulate the Release of Bone Morphogenetic Protein-2 and Accelerate Bone Regeneration. *Biomedicines* **9**, 128 (2021).
81. Babilotte, J. *et al.* Development and characterization of a PLGA-HA composite material to fabricate 3D-printed scaffolds for bone tissue engineering. *Mater. Sci. Eng. C* **118**, 111334 (2021).
82. Nevado, P. *et al.* Preparation and in vitro evaluation of PLA/biphasic calcium phosphate filaments used for fused deposition modelling of scaffolds. *Mater. Sci. Eng. C* **114**, 111013 (2020).
83. Wu, Y. *et al.* 3d printed calcium phosphate cement (CPC) scaffolds for anti-cancer drug delivery. *Pharmaceutics* **12**, 1–15 (2020).
84. Zhang, W. *et al.* Cartilage repair and subchondral bone migration using 3d printing osteochondral composites: A one-year-period study in rabbit trochlea. *Biomed Res. Int.* **2014**, (2014).
85. Chen, Z. *et al.* 3D printing of ceramics: A review. *J. Eur. Ceram. Soc.* **39**, 661–687 (2019).
86. Yan, D. *et al.* Study on the properties of PLA/PBAT composite modified by nanohydroxyapatite. *J. Mater. Res. Technol.* **9**, 11895–11904 (2020).
87. Hassanajili, S., Karami-Pour, A., Oryan, A. & Talaei-Khozani, T. Preparation and characterization of PLA/PCL/HA composite scaffolds using indirect 3D printing for bone tissue engineering. *Mater. Sci. Eng. C* **104**, 109960 (2019).
88. Felfel, R. M. *et al.* In vitro degradation and mechanical properties of PLA-PCL copolymer unit cell scaffolds generated by two-photon polymerization. *Biomed. Mater.* **11**, (2016).
89. Gentile, P., Chiono, V., Carmagnola, I. & Hatton, P. V. An overview of poly(lactic-co-glycolic) Acid (PLGA)-based biomaterials for bone tissue engineering. *Int. J. Mol. Sci.* **15**, 3640–3659 (2014).

90. Ramot, Y., Haim-Zada, M., Domb, A. J. & Nyska, A. Biocompatibility and safety of PLA and its copolymers. *Adv. Drug Deliv. Rev.* **107**, 153–162 (2016).
91. Dwivedi, R. *et al.* Polycaprolactone as biomaterial for bone scaffolds: Review of literature. *J. Oral Biol. Craniofacial Res.* **10**, 381–388 (2020).
92. Deng, X. *et al.* 3D printing of robust and biocompatible poly(ethylene glycol)diacrylate/nano-hydroxyapatite composites via continuous liquid interface production . *J. Mater. Chem. B* 1315–1324 (2021) doi:10.1039/d0tb02182b.
93. Daneshmandi, L., Barajaa, M., Tahmasbi Rad, A., Sydlik, S. A. & Laurencin, C. T. Graphene-Based Biomaterials for Bone Regenerative Engineering: A Comprehensive Review of the Field and Considerations Regarding Biocompatibility and Biodegradation. *Adv. Healthc. Mater.* **10**, 1–25 (2021).
94. Saroia, J. *et al.* A review on biocompatibility nature of hydrogels with 3D printing techniques, tissue engineering application and its future prospective. *Bio-Design Manuf.* **1**, 265–279 (2018).
95. Ee, L. Y. & Li, S. F. Y. Recent advances of 3D printing nanocellulose: structure, preparation and prospects in application. *Nanoscale Adv.* (2021) doi:10.1039/d0na00408a.